Critical Role of cAMP-Dependent Protein Kinase Anchoring to the L-Type Calcium Channel $Ca_v1.2$ via A-Kinase Anchor Protein 150 in Neurons†

Duane D. Hall,*,‡ Monika A. Davare,§,|| Mei Shi,‡ Margaret L. Allen,⊥ Michael Weisenhaus,⊥ G. Stanley McKnight,⊥ and Johannes W. Hell*,‡,§

Department of Pharmacology, Roy J. and Lucille A. Carver College of Medicine, University of Iowa, Iowa City, Iowa 52242-1109, Department of Pharmacology, School of Medicine, University of Wisconsin, Madison, Wisconsin 53706-1532, and Department of Pharmacology, School of Medicine, University of Washington, Seattle, Washington 98195-7750

Received October 25, 2006; Revised Manuscript Received December 4, 2006

ABSTRACT: The cAMP-dependent protein kinase (PKA) regulates a wide array of cellular functions. In brain and heart PKA increases the activity of the L-type Ca^{2+} channel $Ca_v1.2$ in response to β-adrenergic stimulation. $Ca_v1.2$ forms a complex with the β_2-adrenergic receptor, the trimeric G_S protein, adenylyl cyclase, and PKA wherein highly localized signaling occurs [Davare, M. A., Avdonin, V., Hall, D. D., Peden, E. M., Burette, A., Weinberg, R. J., Horne, M. C., Hoshi, T., and Hell, J. W. (2001) *Science 293*, 98−101]. PKA primarily phosphorylates $Ca_v1.2$ on serine 1928 of the central, pore-forming $\alpha_1$1.2 subunit. Here we demonstrate that the A-kinase anchor protein 150 (AKAP150) is critical for PKA-mediated regulation of $Ca_v1.2$ in the brain. AKAP150 and MAP2B specifically co-immunoprecipitate with $Ca_v1.2$ from rat brain. Recombinant AKAP75, the bovine homologue to rat AKAP150, binds directly to three different sites of $\alpha_1$1.2. MAP2B from rat brain also interacts with these same sites in pull-down assays. Gene disruption of AKAP150 in mice dramatically reduces co-immunoprecipitation of PKA with $Ca_v1.2$ and prevents phosphorylation of serine 1928 upon β-adrenergic stimulation in vivo. These results demonstrate the physiological relevance of PKA anchoring by AKAPs in general and AKAP150 specifically in the regulation of $Ca_v1.2$ in vivo.

L-Type Ca^{2+} channels, such as $Ca_v1.2$, substantially contribute to Ca^{2+} influx into neurons (*1*, *2*). These channels regulate membrane excitability (*3*), certain forms of long-term potentiation and long-term depression (*2*, *4*−*7*), and gene expression (*8*, *9*). Regulation of L-type channels is best characterized in the heart where Ca^{2+} influx through $Ca_v1.2$ is crucial for triggering myocardial contraction. During the fight or flight response, β-adrenergic stimulation increases the contractility of the heart in part by enhancing $Ca_v1.2$ channel activity via PKA[1] (*10*−*12*). PKA also upregulates L-type channel activity in neurons (*13*−*17*).

Two different L-type channels have been identified in forebrain neurons, $Ca_v1.2$ and $Ca_v1.3$, previously called class C and class D L-type channels, respectively (*18*−*20*). $Ca_v1.2$ not only is the most prevalent Ca^{2+} channel in the heart but also constitutes ∼80% of the L-type channels in the brain (*2*, *19*, *21*). The central $\alpha_1$1.2 subunit (*18*) forms the ion-conducting pore of $Ca_v1.2$ (*22*). Auxiliary subunits (α_2-δ, -β, and possibly -γ) control different properties of the channel including surface expression and gating kinetics (*22*, *23*). Importantly, only the $\alpha_1$1.2 subunit is required for the PKA-mediated increase in channel activity of $Ca_v1.2$ (*24*). Nevertheless, phosphorylation of the β_2 subunit could contribute to this increase in those $Ca_v1.2$ complexes that contain this isoform of the β subunit (*25*).

The only phosphorylation site for PKA on $\alpha_1$1.2 that is detectable biochemically is serine 1928 (*11*, *20*, *26*−*29*). The phosphorylation level for this site is approximately 17% under basal conditions in the adult rat brain in vivo (*27*). Gao et al. found that mutating serine 1928 to alanine inhibits PKA-mediated phosphorylation of $\alpha_1$1.2 and upregulation of $\alpha_1$1.2 channel activity (*30*). The channel can also be potentiated through proteolytic cleavage of the $\alpha_1$1.2 C-terminus. In neurons, Ca^{2+} influx through NMDA-type glutamate receptors results in cleavage of $\alpha_1$1.2 upstream of serine 1928 by the Ca^{2+}-dependent protease calpain. This cleavage generates a 180 kDa short form of $\alpha_1$1.2 that is 40 kDa smaller than the full-length protein (*31*, *32*). Expression of truncated $\alpha_1$1.2 approximating the calpain cleavage region

† This work was supported by the National Institutes of Health Research Grants RO1-AG017502 and RO1-NS035563 (to J.W.H.), RO1-GM32875 (to G.S.M.), and DA13410 (to G.S.M.). D.D.H. was supported by American Heart Association Scientist Development Grant 0535235N and NIH Training Grants T32 HL07121, T32 DK07759, and T32 AG00213.

* Address correspondence to either author at the University of Iowa. Tel: (319) 384-4732. Fax: (319) 335-8930. E-mail: duane-hall@uiowa.edu; johannes-hell@uiowa.edu.

‡ University of Iowa.

§ University of Wisconsin.

|| Current address: Vollum Institute, Oregon Health Sciences University, Portland, OR 97201.

⊥ University of Washington.

[1] Abbreviations: AKAP, A-kinase anchor protein; AMPA, α-amino-3-hydroxy-5-methylisoxazole-4-propionic acid; β-AR, β-adrenergic receptor; GST, glutathione *S*-transferase; MAP, microtubule-associated protein; NMDA, *N*-methyl-D-aspartate; PAGE, polyacrylamide gel electrophoresis; PKA, cAMP-dependent protein kinase; PCR, polymerase chain reaction; SDS, sodium dodecyl sulfate.

10.1021/bi062217x CCC: $37.00
Published on Web 01/20/2007

yields a channel whose activity is several fold increased compared to full-length $\alpha_1$1.2 (*33*).

PKA targets to various substrate proteins via A-kinase anchor proteins or AKAPs (*34*−*36*). Disruption of the PKA−AKAP interaction inhibits regulation of a number of ion channels by PKA as initially shown for the AMPA-type glutamate receptor (*37*, *38*) and the skeletal muscle L-type channel Ca_v1.1 (*39*). PKA links to Ca_v1.1 through AKAP15/18, recently renamed AKAP7 (*36*), which has also been found to mediate the interaction between PKA and Ca_v1.2 in heart (*40*). In brain, Ca_v1.2 interacts with the microtubule-associated protein MAP2B (*26*), which was the first AKAP identified as such (*41*). However, whether MAP2B or AKAP15/18, which is also expressed in brain (*42*, *43*), or other AKAPs act to anchor PKA at Ca_v1.2 in neurons is unclear.

One such AKAP may be AKAP150, also designated as AKAP5 by the Gene Nomenclature Committee (*36*). AKAP150 is localized to postsynaptic sites of glutamatergic synapses (*44*, *45*) and recruits PKA to the glutamate receptor GluR1 subunit for upregulation of its activity by phosphorylation on serine 845 (*37*, *46*−*49*). Interestingly, both Ca_v1.2 and the β_2-adrenergic receptor (β_2-AR) are also clustered at synaptic sites, where they colocalize for spatially restricted signaling from the β_2-AR to Ca_v1.2 (*31*, *50*). There is evidence of a functional interaction between Ca_v1.2 and AKAP150. Gao et al. observed phosphorylation of Ca_v1.2 by PKA in their cell culture system only when AKAP79, the human homologue of AKAP150, was coexpressed with Ca_v1.2. This phosphorylation was not detectable when mutant AKAP79 deficient for PKA binding was coexpressed (*30*). Furthermore, AKAP79 promotes cell surface expression of Ca_v1.2 in HEK293 cells (*51*). Rodent AKAP150 differs from its human homologue in that it contains 36 imperfect octapeptide repeats of unknown function (*35*). Although the exact mechanism for its effect on Ca_v1.2 surface expression is unknown, collectively these findings indicate that AKAP150 can functionally interact with Ca_v1.2.

Now we show that AKAP150 co-immunoprecipitates with Ca_v1.2 from rat brain. The bovine homologue, AKAP75, binds directly to $\alpha_1$1.2. It specifically interacts with three different sites on $\alpha_1$1.2 (N-terminus, loop I−II, and distal C-terminus) with its strongest binding to the distal C-terminus downstream of serine 1928. These same intracellular domains of $\alpha_1$1.2 mediate its interaction with MAP2B. Stimulation of β-ARs with isoproterenol leads to phosphorylation of $\alpha_1$1.2 on serine 1928 in rats and mice. Importantly, knockout of AKAP150 in mice by gene disruption prevents this phosphorylation in vivo. Accordingly, this β-adrenergic stimulation of serine 1928 phosphorylation establishes for the first time that phosphorylation of this PKA site is regulated in vivo, providing a critical piece of evidence for the functional relevance of serine 1928 phosphorylation. In addition, AKAP150 is the main AKAP that links β-ARs and PKA functionally to Ca_v1.2 in the brain.

EXPERIMENTAL PROCEDURES

Materials. Microcystin LR was obtained from Calbiochem (San Diego, CA) and protein A−Sepharose from Repligen. Protein G−Sepharose and glutathione−Sepharose were purchased from Amersham Pharmacia. Other reagents were of standard biochemical quality and were obtained from the usual commercial suppliers.

Antibodies. The following antibodies were previously described. The anti-$\alpha_1$1.2 antibody was raised against a GST-fusion protein spanning parts of the cytosolic loop between domains II and III of $\alpha_1$1.2 (*26*). The phosphospecific antibody CH1923-1932P (anti-$\alpha_1$1.2-P) was made against a peptide with the indicated residues upstream and downstream of the phosphorylated serine 1928 (*11*, *26*). Control antibodies to test for nonspecific immunoprecipitation were nonimmune purified rabbit and mouse IgG from Zymed Laboratories, Inc. (South San Francisco, CA) and Jackson ImmunoResearch Laboratories, Inc. (West Grove, PA), respectively. Antibodies against the PKA regulatory subunits RIIα and RIIβ were as described in ref *52*. The anti-AKAP15 antibody was generously provided by Dr. W. A. Catterall (University of Washington, Seattle, WA) (*43*), anti-GST by Dr. J. W. Tracy (University of Wisconsin, Madison, WI) (*53*), and the antibody against the catalytic PKA Cα subunit by Dr. C. S. Rubin (Albert Einstein College of Medicine, Bronx, NY) as described earlier (*26*). Antibodies against human AKAP79 (clone 22) (*54*, *55*), MAP2B (clone 18) (*26*), and Yotiao (AKAP350/450, clone 7) were purchased from Transduction Laboratories (Lexington, KY), mAKAP (*56*, *57*) and polyclonal rodent AKAP150 was from Upstate (Lake Placid, NY) (*26*).

Administration of Isoproterenol and Propranolol. Two-month-old rats or mice were intraperitoneally injected with 1 mL of either vehicle (PBS), 10 mg/kg isoproterenol, or isoproterenol plus 10 mg/kg propranolol. To minimize distress and inadvertent activation of adrenergic signaling pathways, animals were handled by an experienced experimenter who was observed by a neutral person. Each animal was gently held against the chest and oriented for easy access to the abdomen for injection. Only animals that did not or only slightly flinch were used for experiments. After 20−30 min, as indicated, animals were euthanized and decapitated. All procedures were in accordance with the Animal Welfare Act of the United States and the recommendations by the Panel on Euthanasia of the American Veterinary Association.

Immunoprecipitation and Immunoblotting. Brain tissue was harvested immediately after decapitation from male Harlan Sprague-Dawley rats, male Taconic C57black/6 mice, or AKAP150 knockout mice, which were congenic with the former due to seven cross-breedings. Forebrains including the cortex and hippocampus were isolated and homogenized at 1 mL/100 mg tissue in ice-cold buffer including 320 mM sucrose, 10 mM Tris-HCl, pH 7.4, 10 mM EGTA, and 10 mM EDTA supplemented with protease inhibitors (1 μg/mL pepstatin A, 10 μg/mL leupeptin, 20 μg/mL aprotinin, 200 nM phenylmethanesulfonyl fluoride, 8 μg/mL calpain inhibitor I, and 8 μg/mL calpain inhibitor II) and phosphatase inhibitors (1 mM *p*-nitrophenyl phosphate, 50 mM NaF, 20 mM sodium pyrophosphate, and 4 μM microcystin LR), as described elsewhere (*26*, *28*). These phosphatase inhibitors block dephosphorylation of $\alpha_1$1.2 throughout the procedure (*29*). Supernatants were recovered from a low-speed spin (2 min, 5000*g* in a Sorvall SS-34 rotor) to remove debris and then subjected to ultracentrifugation (30 min, 250000*g* in a Beckman Ti-50 rotor) to pellet membranes. Membranes were solubilized and homogenized in 1% Triton X-100, 10 mM

Table 1: PCR Primers Used for Generating GST-Fusion Proteins[a]

fusion	residues	PCR primers
$\alpha_1$1.2 CT-B	1694−1817 (1724−1847)	forward: 5′-CGG CAA GGA TCC GTC GAC GAC ATC TTC AGG AGG GCT GGA GG-3′ reverse: 5′-GGC TGA ATT C*CG TAG AAT CGA GAC CGA GGA GAC CGT TAG GGA TAG GCT TAC C*GT GGC ACC TCT TAG AGC TGA G-3′
$\alpha_1$1.2 CT-C	1804−1927 (1834−1957)	forward: 5′-GCC GTC GGA TCC GTC GAC GTA CAG GAG GCA GCA TGG AAA CTC-3′ reverse: 5′-GGC TGA ATT C *CG TAG AAT CGA GAC CGA GGA GAC CGT TAG GGA TAG GCT TAC C*GT GAT GAA CCA GAT GCA AGG GC-3′
$\alpha_1$1.2 CT-D	1914−2037 (1944−2067)	forward: 5′-CGC AGA GGA TCC GTC GAC ATC TCT CAG AAG ACA GCC TTG C-3′ reverse: 5′-GGC TGA ATT C *CG TAG AAT CGA GAC CGA GGA GAC CGT TAG GGA TAG GCT TAC C*CA GGC TGC TGG CGC TGC CG-3′
$\alpha_1$1.2 CT-E	2024−2140 (2054−2171)	forward: 5′-CCG AGA GGA TCC GTC GAC GGA GCT CCA GGC AGA CAG TTC C-3′ reverse: 5′-GGC TGA ATT C *CG TAG AAT CGA GAC CGA GGA GAC CGT TAG GGA TAG GCT TAC C*CA GGT TGC TGA CAT AGG ACC TGC-3′
AKAP75	1−428	forward: 5′-GCG AAT GGA TCC ATG GAG ATC ACA GTT TCT GAA ATA C-3′ reverse: 5′-GCG AGT CGA CGA ATT CA*G GCG TAG TCT GGG ACG TCG TAT GGG TA*C TGT AGA CGA TTG TTT ATT GTA TTA TC-3′

[a] Amino acid residues are designated for rat $\alpha_1$1.2. Homologous rabbit $\alpha_1$1.2 sequences are in parentheses. Residues for bovine AKAP75 are for the full-length protein. Italicized primer sequences encode for a V5 epitope tag ($\alpha_1$1.2 fusion proteins) or an HA tag (AKAP75).

Tris-HCl, pH 7.4, 20 mM EDTA, and 10 mM EGTA supplemented with protease and phosphatase inhibitors in the same volume used above. After ultracentrifugation to sediment nonsolubilized material, $\alpha_1$1.2 was immunoprecipitated from the supernatants with a near-saturating concentration of affinity-purified anti-$\alpha_1$1.2 [10 μg in 500 μL (*19*, *20*)] before immunoblotting with various antibodies. Control immunoprecipitations were performed with purified rabbit IgG that originated from naive, i.e., nonimmunized, animals. Total extract (20 μL; 5% of volume used for immunoprecipitation) was loaded in parallel on most gels to test whether the commercial antibodies against the different AKAPs detect the expected antigen in brain.

To quantitatively evaluate serine 1928 phosphorylation in the in vivo experiments, blots were first probed with anti-$\alpha_1$1.2-P and subsequently with anti-$\alpha_1$1.2 to correct for variability in the amount of total $\alpha_1$1.2. The ratio of the anti-$\alpha_1$1.2-P to the anti-$\alpha_1$1.2 signal was determined for each sample by densitometry. Ratios were normalized to the ratio of the vehicle control injected animals within each experiment to allow comparison between experiments (*27*). Averages and errors (SEMs) were calculated. Values were assumed to be significantly different if $p < 0.05$ (paired *t*-test). Immunoblot signals were within the linear range for all experiments as we recently described (*27*, *58*).

Production of GST-Fusion Protein Vectors. Rat $\alpha_1$1.2 cDNA (*59*) (Genbank accession number M67515) served as a template for the production of fragments of the $\alpha_1$1.2 C-terminus as GST-fusion proteins. Primers used for PCR amplification are described in Table 1. 5′ forward primers carried a *Bam*HI restriction site. The 3′ reverse primers contained an *Eco*RI restriction site and a V5 epitope tag followed by the $\alpha_1$1.2 specific sequence. For GST-AKAP75 construction, pCIS2/AKAP75 was used as a template (*60*) with a *Bam*HI site-containing forward primer and a *Sal*I + *Eco*RI site-containing reverse primer with the sequence encoding the HA epitope tag (Table 1). Fragments were amplified with the HF-Advantage PCR kit from Clontech, purified with the PCR purification kit from QIAGEN, digested with *Bam*HI and *Eco*RI, and ligated into *Bam*HI/*Eco*RI-treated pGEX4T1. Positive clones were confirmed by sequencing. The GST-fusion constructs CT-1 (rabbit $\alpha_1$1.2 residues 1507−1733; Genbank accession number A33546), CT-5 (residues 1509−1622), and CT-7 (residues 2030−2171) were kindly provided by Dr. M. M. Hosey (Northwestern University, Chicago, IL) (*61*).

In Vitro Pull-Down Assays with GST-Fusion Proteins. GST-fusion proteins of $\alpha_1$1.2 were expressed and affinity-purified from Nova Blue (Novagen, Madison, WI) and BL21 Star (Invitrogen, San Diego, CA) *Escherichia coli* strains and used for pull-down assays as described previously (*28*, *53*, *62*). GST fusions of $\alpha_1$1.2 fragments were immobilized on glutathione−Sepharose, washed, and incubated with bacterially expressed 6×His-tagged AKAP75 (*63*) or brain cytosol as a source of MAP2B before immunoblotting with antibodies against AKAP79 or MAP2B. GST-fusion proteins were analyzed in parallel immunoblots with anti-GST antibodies to monitor relative amounts and degree of degradation. To obtain a cytosolic brain fraction one rat forebrain (~1 g) was homogenized in 10 mL of ice-cold sucrose buffer as above followed by removal of particulate material by ultracentrifugation (30 min, 250000*g* in a Beckman Ti-50 rotor).

Dot Blot Overlay Assays with GST-Fusion Proteins. GST-fusion proteins were affinity purified from *E. coli* lysates on glutathione−Sepharose, eluted with 15 mM glutathione, and dialyzed against TBS (10 mM Tris-HCl, pH 7.4, 150 mM NaCl) to remove glutathione. Protein concentrations were determined with a Bradford assay (Bio-Rad, Hercules, CA) and 0.5 μg of fusion proteins or GST alone spotted onto polyvinyl difluoride membranes under vacuum. GST-AKAP75 was affinity purified on glutathione−Sepharose, eluted with 15 mM glutathione at pH 8.5, dialyzed, and applied to the dot blots at 100 nM. After washing, AKAP75 was detected by incubating dot blots with the rodent anti-AKAP150 antibody, followed by the horseradish peroxidase-coupled anti-rabbit IgG secondary antibody and detection with the ECL reagent (Amersham) by film exposure. The quality of each GST-fusion protein was monitored in parallel by SDS−PAGE and immunoblotting with anti-GST antibodies.

Generation of AKAP150 KO Mice. The AKAP150 gene was disrupted by replacing the entire coding sequence of AKAP150 with a neomycin phosphotransferase cassette by homologous recombination in embryonic stem cells (Weisenhaus, Allen, and McKnight, manuscript in preparation). AKAP150−/− mice were generated in a 129S1/SvImJ background (Jackson Laboratories, Bar Harbor, ME) and then

back-bred seven times into a C57BL/6 background (Taconic Farms Inc., Germantown, NY) prior to study. Genotyping of animals was performed by amplifying the 5′ region of AKAP150 or the neomycin cassette from genomic DNA isolated from tail clips. For the AKAP150 PCR the forward primer was 5′-AGA CCA GCG TTT CTG AG-3′ and the reverse primer 5′-TTC CTG TGT GTC ACA AG-3′. For the neomycin PCR, the forward primer was 5′-TCG CAT GAT TGA ACA AG-3′ and the reverse primer 5′-AAG CAC GAG GAA GCG GT-3′. The knockout and wild-type mice used in these studies were littermates obtained from heterozygous mating.

Cyclic AMP Assays from Cortical Slices. Brains from 2−3-month-old mice were immediately harvested after decapitation and chilled in ice-cold ACSF buffer (120 mM NaCl, 10 mM TEA-HCl, 5.4 mM $CsCl_2$, 1 mM $CaCl_2$, 2 mM $MgCl_2$, 10 mM HEPES, pH 7.3, 5 mM glucose). Cortical slices were prepared with a Leica VT 100S vibratome to a thickness of 350 μm and incubated in ACSF buffer at 32 °C for 30 min and then at room temperature for 30 min before being transferred to modified ACSF buffer (120 mM NaCl, 10 mM TEA-HCl, 5.4 mM $CsCl_2$, 2.2 mM $CaCl_2$, 1 mM $MgCl_2$, 10 mM HEPES, pH 7.3, 5 mM glucose) for 30 min at room temperature. Slices were pretreated with 3 μM propranolol in modified ACSF 30 min prior to addition of other drugs (3 μM isoproterenol, 50 μM forskolin, 50 μM dideoxyforskolin, or DMSO vehicle) for 10 min. Slices were then immediately frozen.

The cAMP Correlate enzyme immunoassay kit (Assay Designs, Ann Arbor, MI) was used to measure cAMP levels from treated slices according to the manufacturer's protocol. Briefly, slices were homogenized in 0.1 N HCl and cleared by centrifugation at 1000*g*. Protein concentrations were determined using a BCA protein assay (Pierce, Rockford, IL), and approximately 40 μg was used per reaction. This concentration was found to reliably give cAMP levels that fell within the cAMP standard curve for all treatments. Cyclic AMP levels as determined from the cAMP assay were normalized to protein content from the BCA assay (Pierce) for each sample. Statistical significance was determined using Prism 4.0 (GraphPad Software, San Diego, CA) by performing a two-tailed *t*-test on averages ± SEM.

RESULTS

β-Adrenergic Stimulation of Serine 1928 Phosphorylation. One of the classic biological signaling pathways is the upregulation of L-type Ca^{2+} channel activity upon activation of β-ARs. This pathway was originally characterized in the heart (*10*−*12*) and has been found to be widespread in brain (*13*, *14*, *16*, *50*). For highly localized signaling, $Ca_v1.2$ constitutively associates with the β_2-AR and PKA to efficiently respond to β-adrenergic activation (*50*). We tested whether β-adrenergic stimulation in vivo leads to phosphorylation of serine 1928, the main PKA site on $\alpha_1$1.2. The β-adrenergic agonist isoproterenol was intraperitoneally injected into 2-month-old rats. If animals flinched or showed other signs of stress, they were not included in the study since adrenergic pathways could have been activated independent of injection. After 30 min animals were euthanized, and forebrains were immediately harvested and homogenized on ice. The $\alpha_1$1.2 subunit was extracted from Triton X-100 solubilized membranes, immunoprecipitated, and analyzed via immunoblotting. The phosphospecific antibody anti-$\alpha_1$1.2-P was used to detect serine 1928 phosphorylation and the anti-$\alpha_1$1.2 antibody to monitor total $\alpha_1$1.2 levels. As previously characterized (*12*), anti-$\alpha_1$1.2-P only recognizes the full length $\alpha_1$1.2 but not the truncated short form, which is lacking serine 1928 (Figure 1A; see also Figure 4A). Administration of isoproterenol resulted in a significant increase in serine 1928 phosphorylation as compared to vehicle control (Figure 1B). Coadministration of the β-adrenergic antagonist propranolol prevented this increase, thereby demonstrating that the isoproterenol effect was specifically mediated by β-ARs. These results show for the first time that phosphorylation of serine 1928 is regulated in vivo by this classic β-adrenergic signaling pathway that is crucial for $Ca_v1.2$ regulation. This finding further defines this site as a critical PKA site thought to principally mediate the PKA effect on $Ca_v1.2$ (*11*, *20*, *26*−*30*).

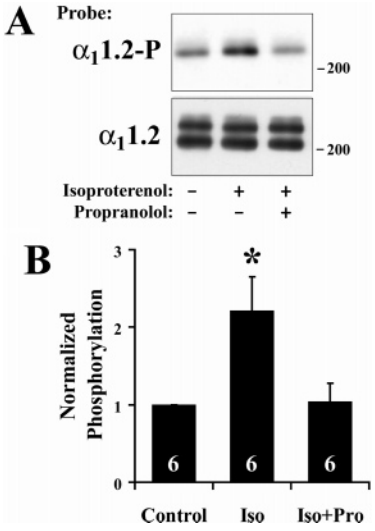

FIGURE 1: Isoproterenol upregulates $Ca_v1.2$ phosphorylation on serine 1928 of the $\alpha_1$1.2 subunit in vivo. Two-month-old rats were intraperitoneally injected under stress-free conditions and without sign of distress with 1 mL of vehicle (PBS), (−)-isoproterenol (10 mg/kg), or (−)-isoproterenol plus (*S*)-(−)-propranolol (10 mg/kg). After 30 min, rats were decapitated, and forebrain material was immediately harvested and homogenized as described in Experimental Procedures. The $\alpha_1$1.2 subunit of $Ca_v1.2$ was immunoprecipitated from Triton X-100 solubilized membranes with the anti-$\alpha_1$1.2 antibody in the presence of phosphatase inhibitors, which preserve the phosphorylation status of $\alpha_1$1.2. (A) Immunoblots were probed with phosphospecific anti-$\alpha_1$1.2-P recognizing phosphorylated serine 1928 (top) and, after stripping, reprobed with the anti-$\alpha_1$1.2 to determine relative $\alpha_1$1.2 immunoprecipitated in each sample (bottom). (B) Quantification of immunoblot signals through densitometry. The ratios of the anti-$\alpha_1$1.2-P to the anti-$\alpha_1$1.2 immunosignals for each sample were calculated and normalized to the control ratio for each set of rats. Isoproterenol significantly increased serine 1928 phosphorylation (*, $p < 0.05$, SEM, *t*-test). The number of rats treated in three independent experiments is indicated within bars on the graph.

AKAP150 Is Associated with $Ca_v1.2$ in Brain. It is likely that PKA-dependent phosphorylation of $Ca_v1.2$ requires an interaction with an AKAP. We hypothesized that AKAP75/79/150 may serve as this AKAP since $Ca_v1.2$, the β_2-AR, and AKAP150 are all enriched at postsynaptic sites (*31*, *44*, *45*, *50*). AKAP150 links PKA to the AMPA receptor GluR1 subunit (*37*, *46*, *49*) in neurons. It is also known that the

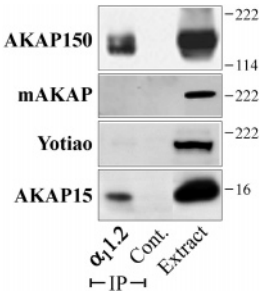

FIGURE 2: AKAP150 and AKAP15 but not mAKAP or Yotiao are associated with $Ca_v1.2$. Forebrains from 2−4-month-old rats were isolated and homogenized as described in Experimental Procedures. The $\alpha_1$1.2 subunit of $Ca_v1.2$ and nonspecific proteins were immunoprecipitated from Triton X-100 solubilized membranes with anti-$\alpha_1$1.2 and control IgG, respectively. The resulting precipitates (lanes 1 and 2) and total membrane extracts (5% input; lane 3) were analyzed by immunoblotting with antibodies against AKAP150, mAKAP, Yotiao, and AKAP15. All four AKAPs showed strong immunoreactive bands of the expected molecular masses in the extract samples. AKAP150 and AKAP15 but not mAKAP or Yotiao specifically copurified with $Ca_v1.2$. Comparable results were obtained in several experiments.

increase in phosphorylation of $Ca_v1.2$ by PKA described by Gao et al. in transfected HEK293 cells upon activation of PKA was seen only when wild-type human AKAP79 was also ectopically expressed (*30*). Furthermore, AKAP79 fosters expression of $Ca_v1.2$ at the plasma membrane in transfected HEK293 cells (*51*). We had previously observed that AKAP150 did not copurify with $\alpha_1$1.2 from brain homogenates during our initial characterization of the interaction of $\alpha_1$1.2 with MAP2B (*26*). These studies had been performed without including NaCl in the homogenization buffer. NaCl may aid in solubilizing proteins and in stabilizing protein interactions. We therefore tested whether AKAP150 is associated with $Ca_v1.2$ after solubilization of $Ca_v1.2$ with 1% Triton X-100 in the presence of 150 mM NaCl. We then reproducibly obtained co-immunoprecipitation of AKAP150 with the $\alpha_1$1.2 subunit of $Ca_v1.2$ (Figure 2).

AKAP15 but Not mAKAP or Yotiao Is Associated with $Ca_v1.2$ in Brain. We also tested whether other AKAPs would co-immunoprecipitate with $Ca_v1.2$ under our conditions, including AKAP15/18, mAKAP [originally AKAP100 (*64*)], and Yotiao. AKAP15 binds to a leucine zipper-like region on $\alpha_1$1.2 (*40*). Functionally, it has been shown that AKAP15 can recruit PKA to the $Ca_v1.2$ complex in heart and upon ectopic expression in HEK293 cells (*40*, *42*, *43*, *65*). AKAP15 is also expressed in brain, and we found that it co-immunoprecipitated with $\alpha_1$1.2 from rat brain extract (Figure 2).

mAKAP recruits PKA to the cardiac ryanodine receptor (type 2) via an interaction with a leucine zipper-like motif (*66*). The ryanodine receptor is exactly juxtaposed to $Ca_v1.2$ in the plasma membrane, which triggers Ca^{2+}-induced Ca^{2+} release from the sarcoplasmic reticulum by the ryanodine receptor. Like $Ca_v1.2$, ryanodine receptors are also present in dendritic spines as indicated by immunohistochemical localization studies (*67*, *68*) and by Ca^{2+} imaging (*69*, *70*). Electrophysiological recordings indicate that $Ca_v1.2$ is functionally coupled to ryanodine receptors in neurons (*71*). The spatial proximity of ryanodine receptors and $Ca_v1.2$ puts ryanodine receptor-associated mAKAP into the immediate vicinity of $Ca_v1.2$ in cardiomyocytes. We therefore investigated whether mAKAP would interact with $Ca_v1.2$ in forebrain lysates. Although mAKAP is prominent in brain (Figure 2, lysate lane), it did not co-immunoprecipitate with $\alpha_1$1.2.

The AKAP Yotiao is an ~230 kDa splice form of AKAP350/450 and links PKA and PP1 to the NMDA-type glutamate receptor at postsynaptic sites (*72*, *73*). Because both $Ca_v1.2$ and the NMDA receptor are concentrated at postsynaptic sites and overlap in their subcellular distribution, we evaluated whether Yotiao is associated with $\alpha_1$1.2, with negative results (Figure 2). We showed earlier that AKAP220 is also not detectable in $\alpha_1$1.2 immunoprecipitates (*26*). Concerned that this interaction was not observed due to the lack of NaCl as with AKAP150 above, we investigated this potential interaction with 150 mM NaCl present and now confirm our previous negative results (data not shown).

Similarly, our initial interaction of MAP2B with $Ca_v1.2$ (*26*) may have been facilitated in the absence of NaCl. We therefore re-evaluated the association of MAP2B with $Ca_v1.2$ in the presence of NaCl. MAP2B co-immunoprecipitated with $Ca_v1.2$ from brain extracts of young (postnatal day 5) and adult (older than 3 months) rats (Figure 3). MAP2C is a juvenile splice form of MAP2B, which is mainly expressed in young rats and lacks the central 1363 residues of MAP2B. It does contain the PKA binding site near the N-terminus and the three microtubule binding segments near the C-terminus (Figure 3). MAP2C, which was easily detectable in brain extracts from 5-day-old rats, did not coprecipitate with $Ca_v1.2$. The lack of interaction of MAP2C with $\alpha_1$1.2 suggests that the central MAP2B region is critical for binding to $Ca_v1.2$. The absence of co-immunoprecipitation of mAKAP, Yotiao, AKAP220, and MAP2C with $Ca_v1.2$ demonstrates that the observed interactions with AKAP150, AKAP15, and MAP2B are specific for these AKAPs.

AKAP75 and MAP2B Directly Bind to Three Different Segments of $\alpha_1$1.2. To determine whether AKAP75/79/150 and MAP2B interact directly with $\alpha_1$1.2, we performed pull-down experiments with GST-fusion proteins covering the N- and C-terminus as well as the large intracellular loops between domains I−IV (loops I−II, II−III, and III−IV). We used recombinant 6×His-tagged bovine AKAP75 expressed in *E. coli* for these pull-down assays as AKAP150 proved difficult to express. AKAP75 shares a high degree of homology with rodent AKAP150 but lacks the 36 imperfect octapeptide repeats of unknown function present in AKAP150 (*35*). We utilized the cytosolic fraction of forebrain lysate as a source of native MAP2B as we were not able to express MAP2B or several of its fragments in *E. coli*. Both recombinant AKAP75 and forebrain MAP2B showed specific binding to the N-terminus, loop I−II, and the long C-terminal fragment that started about 150 residues downstream of the last transmembrane segment (Figure 4A,B). No interaction was detected with bound GST alone or glutathione−Sepharose, which was otherwise used to immobilize the GST-fusion proteins. The relative amounts of the GST-fusion proteins were monitored by separate immunoblots (Figure 4B, bottom). Note that expression of GST-loop I−II and GST-C-Term was usually lower than that of all the other GST-fusion proteins. The amount of GST-N-Term was typically comparable to most other fusion proteins and is higher than usual in the immunoblot depicted in Figure

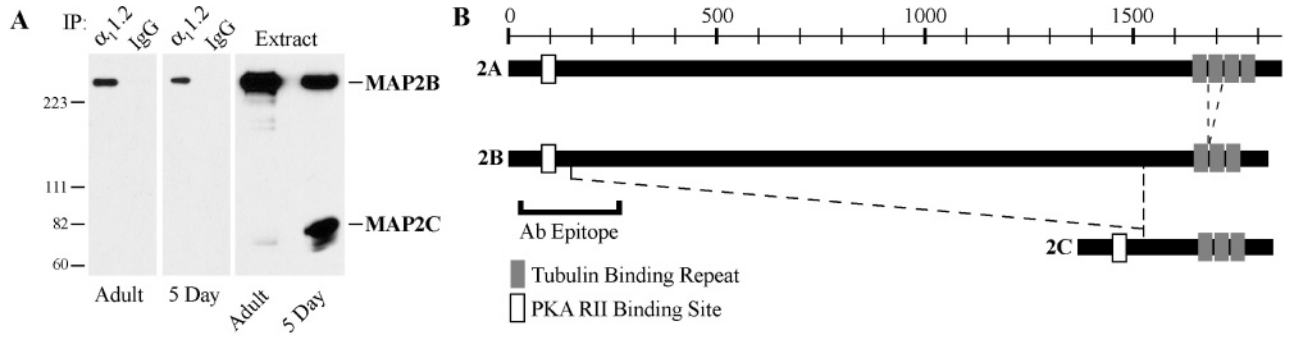

FIGURE 3: MAP2B but not MAP2C is bound to $Ca_v1.2$. Rat forebrains from 5-day-old juvenile rats and 4−6-month-old adult rats were isolated and homogenized as described in Experimental Procedures. The $\alpha_1$1.2 subunit of $Ca_v1.2$ and nonspecific proteins were immunoprecipitated from Triton X-100 solubilized membranes with anti-$\alpha_1$1.2 or control IgG, respectively, and immunoblotted with antibodies against MAP2B (A). The anti-MAP2B antibody had been produced against the N-terminal region of MAP2B [labeled Ab Epitope in (B)] though it recognizes other MAP2 isoforms including MAP2C (*85*) as demonstrated here by immunoblotting of 5-day-old brain extracts (A, right panel). MAP2C is devoid of 1363 residues present in the middle of MAP2B (*85*). It contains the binding site for the regulatory subunit of PKA (RII) near the N-terminus (*86*, *87*) and the three microtubule binding segments near the C-terminus (B) (*88*, *89*). MAP2C migrates with an apparent molecular mass of ~70 kDa and is mainly expressed in 5-day-old rats but is barely visible in adult rats (A, right panel). In contrast to MAP2B, MAP2C was not detectable in immunopurified $Ca_v1.2$ complexes (A, left and middle panels). Three experiments yielded similar results.

4B. Accordingly, AKAP75 and MAP2B binding to all three GST-fusion proteins, i.e., N-Term, loop I−II, and C-Term, is specific for these sequences.

We cannot be certain that MAP2B bound directly to one, two, or all three $\alpha_1$1.2 fragments because other proteins in the forebrain extract could have mediated this interaction. However, the observation that MAP2B binding showed the same pattern as AKAP75 binding suggests similar $\alpha_1$1.2 binding mechanisms for the two proteins. AKAP75 binding is most likely direct as we used recombinant AKAP75 expressed in *E. coli*. In addition, we found earlier that MAP2B directly associates with $\alpha_1$1.2 purified to homogeneity by double immunoprecipitation (*26*). Collectively, these results support a direct interaction between MAP2B and $\alpha_1$1.2.

The N-terminus and loop I−II are rather short (~120 residues), but the C-terminus is more than 600 residues long. To narrow down the AKAP75 binding site within this region, affinity-purified GST-fusion proteins of shorter, overlapping $\alpha_1$1.2 C-terminal segments (Figure 4C) were used in a dot blot overlay assay. The different GST-fusion proteins were affinity purified and vacuum spotted onto polyvinyl difluoride membranes. Membranes were incubated sequentially with 100 nM affinity-purified GST-tagged AKAP75 (Figure 4D, right panel), anti-AKAP150 antibodies, and HRP-coupled secondary anti-rabbit IgG antibodies for detection by chemilluminescence.

AKAP75 reproducibly showed the strongest interaction with CT-7 (rabbit $\alpha_1$1.2 residues 2030−2171) and, to a lesser degree, CT-E (rat $\alpha_1$1.2 residues 2024−2140) (Figure 4D, top panel). Other fusion proteins typically exhibited signals near the background level as determined with GST alone. Although GST has a tendency to dimerize in solution, we did not detect an interaction between GST-AKAP75 and GST alone in this overlay assay. Therefore, this assay permits detection of specific interactions between AKAP75 and $\alpha_1$1.2-derived GST-fusion proteins. Stripping and reprobing with anti-GST illustrated that comparable amounts of each GST-fusion protein had been spotted onto the membranes (Figure 4D, middle panel). The quality of each fusion protein was monitored by immunoblotting with anti-GST (Figure 4D, bottom panel). CT-7 spans the last 142 and CT-E the last 117 residues of rabbit and rat $\alpha_1$1.2, respectively. According to the results in Figure 4B,D, binding of AKAP75 to $\alpha_1$1.2 is direct and mediated by three sites, the N-terminus (residues 1−124), loop I (residues 409−526), and the distal C-terminus.

Deletion of the AKAP150 Gene Abrogates Stimulation of $\alpha_1$1.2 Phosphorylation on Serine 1928 in Vivo. In order to test whether the above interactions between AKAP75/79/150 and $\alpha_1$1.2 had functional consequences, we eliminated AKAP150 expression in mice by targeted gene disruption. Genotypes were confirmed through PCR analysis (Figure 5A). Immunoblotting showed that the AKAP150 band at an apparent molecular mass of 150 kDa is prominent in forebrain homogenates from wild-type mice but completely absent in lysates from AKAP150 KO mice, as expected (Figure 5B, second panel). AKAP150 was also undetectable in $\alpha_1$1.2 immunoprecipitates from KO animals (Figure 5D). Differences in the expression of PKA subunits or other AKAPs were not readily detectable as the levels of MAP2B, AKAP15, PKA-RIIα, PKA-RIIβ, or PKA-C remained similar between wild-type and AKAP150 KO forebrain extracts (Figure 5B). However, there was an 80% reduction in the relative amount of the catalytic subunit of PKA (PKA-C) that specifically co-immunoprecipitated with $\alpha_1$1.2 from AKAP150 KO versus wild-type mouse forebrain (Figure 5C). There was little to no PKA-C immunosignal in immunoprecipitates with control antibodies. We conclude that in rodent brain AKAP150 is important for anchoring the majority of PKA to $Ca_v1.2$.

To test whether AKAP150 is necessary for regulating $\alpha_1$1.2 phosphorylation by PKA in vivo, we injected the β-adrenergic agonist isoproterenol intraperitoneally into mice in a manner that caused little to no stress as described above for rats. After 20 min animals were euthanized, forebrains were immediately harvested, and $\alpha_1$1.2 was immunoprecipitated from solubilized membranes. Subsequent immunoblotting with anti-$\alpha_1$1.2-P showed an approximately 2-fold increase in $\alpha_1$1.2 serine 1928 phosphorylation in wild-type mice over vehicle-injected mice (Figure 6). Coadministration of the β-adrenergic antagonist propranolol prevented this

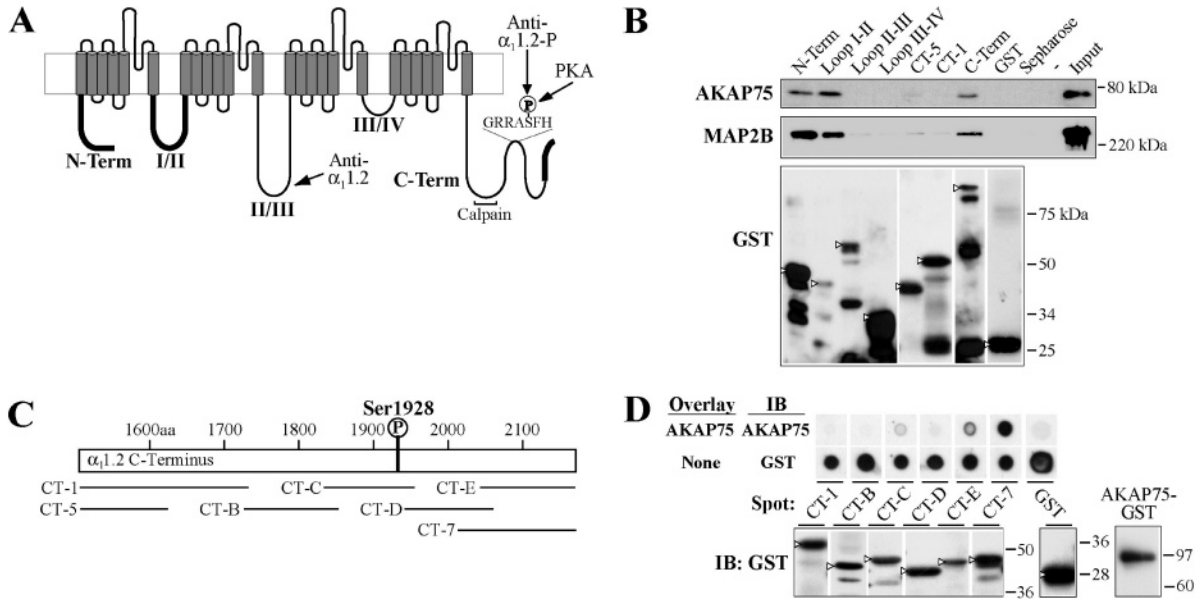

FIGURE 4: AKAP75 and MAP2B bind to the N-terminus, loop I−II, and C-terminus of the $\alpha_1$1.2 subunit of Ca_v1.2. (A) Schematic depiction of the $\alpha_1$1.2 subunit of Ca_v1.2. AKAP75 and MAP2B binding sites on $\alpha_1$1.2 [N- and C-terminus and loop I−II; see (B) and (D)] are highlighted by bold lines. The epitopes for the anti-$\alpha_1$1.2 antibody in loop II−III and the phosphospecific anti-$\alpha_1$1.2-P antibody surrounding serine 1928, which constitutes the PKA phosphorylation site, are indicated. The region where calpain cleaves $\alpha_1$1.2 (*31*) is indicated by a horizontal bracket. This cleavage removes serine 1928 as well as the AKAP150/MAP2B binding site that is in the distal C-terminus. (B) Pull-down assays of AKAP75 and MAP2B with $\alpha_1$1.2 GST-fusion proteins. Fusion proteins of the N-terminus (N-Term), the loops between the four domains (loop I−II, II−III, and III−IV), and three regions of the C-terminus (CT-1, residues 1507−1733; CT-5, residues 1509−1622; C-Term, residues 1584−2140 of $\alpha_1$1.2) were expressed in *E. coli*, adsorbed onto glutathione−Sepharose, and incubated with lysate from *E. coli* expressing 6×His-tagged bovine AKAP75 or with cytosolic brain extract as a source of MAP2B. Immunoblotting with antibodies against human AKAP79 and MAP2B showed that both AKAPs specifically bound to the N- and C-terminus and loop I−II (top two panels). GST protein levels were analyzed by immunoblotting with anti-GST antibodies (bottom panel; arrowheads indicate the position of the respective full-length GST-fusion protein; lanes are rearranged to match the loading order of the immunoblots shown in the top panels). Cytosolic brain extract or *E. coli* lysate (5% of input each) was loaded in parallel as a positive control for MAP2B and AKAP75 probing (Input). (C) Depiction of the $\alpha_1$1.2 C-terminus starting immediately after the last transmembrane region and relative positions of smaller GST-fusion proteins used to narrow the AKAP75 binding site. (D) The illustrated GST-fusion proteins in (C) were expressed in *E. coli*, affinity purified on glutathione−Sepharose, eluted with glutathione, and dialyzed. Fusion proteins, 0.5 μg, were vacuum spotted onto polyvinyl difluoride membranes. Membranes were subsequently incubated with 100 nM affinity-purified GST-tagged AKAP75, the anti-AKAP150 antibody, and a horseradish peroxidase-coupled anti-rabbit IgG antibody, which was detected by chemiluminescence. CT-7 and, to a lesser degree, CT-E specifically interacted with AKAP75 (D, top panel). CT-7 and CT-E cover the last 142 and 117 residues of $\alpha_1$1.2, respectively. Other fusion proteins and GST did not show specific stainings. Dot blots were stripped and reprobed with anti-GST to show relative amounts of each GST-fusion protein spotted onto the membranes (D, middle panel). All dots are from the same blot and exposure but rearranged for ease of viewing. To exclude against degradation, the fusion proteins were analyzed by separate immunoblotting with anti-GST antibodies (D, bottom panel; lanes were rearranged for clarity). An immunoblot of the GST-AKAP75 used for the overlay assays is shown on the right. Similar observations were made in three (D) or four (B) experiments.

increase, demonstrating that the isoproterenol effect was mediated by β-ARs. Disruption of AKAP150 prevented this isoproterenol-dependent increase in serine 1928 phosphorylation.

According to our model, dislocation of PKA anchoring from Ca_v1.2 is sufficient to explain the lack of an isoproterenol-dependent effect on serine 1928 phosphorylation in the AKAP150 KO mice. AKAP150 is known to bind to the β_2-AR (*74*) as well as bind to and negatively regulate adenylyl cyclase types V/VI (*75*). It is conceivable that AKAP150 elimination may alter surface localization of the β_2-AR and therefore cAMP production in neurons. To determine the capacity of AKAP150 KO neurons to produce cAMP, cAMP assays were performed on acute cortical slices. As can be seen in Figure 6C, basal cAMP levels were similar in wild-type and KO slices (vehicle control). Isoproterenol significantly increased cAMP levels 2-fold in both genetic backgrounds while pretreatment of slices with propranolol blocked the isoproterenol-dependent increase in cAMP. To assess the total capacity of slices to produce cAMP, the adenylyl cyclase activator forskolin, or its inactive analogue dideoxyforskolin (DDF), was incubated with the cortical slices. Forskolin significantly increased cAMP approximately 3-fold while DDF had no effect. Again, there was no difference between wild-type and KO cAMP levels for either treatment. Accordingly, we find no difference in cAMP production between wild-type and AKAP150 KO neurons either basally or in response to adrenergic and adenylyl cyclase agonists. These data support a model in which AKAP150 is critical for anchoring of PKA on Ca_v1.2 whereas any potential effect on surface localization of the β_2-AR plays a minor, if any, role in this regulation of Ca_v1.2 phosphorylation.

DISCUSSION

Our results demonstrate that activation of the β-adrenergic signaling cascade in intact animals results in increased phosphorylation of the neuronal Ca_v1.2 L-type calcium channel on serine 1928 of the $\alpha_1$1.2 subunit. The increase in phosphorylation on serine 1928 in response to isoproterenol depends on anchoring of PKA through AKAP150 by binding to three intracellular domains of $\alpha_1$1.2. Other AKAPs

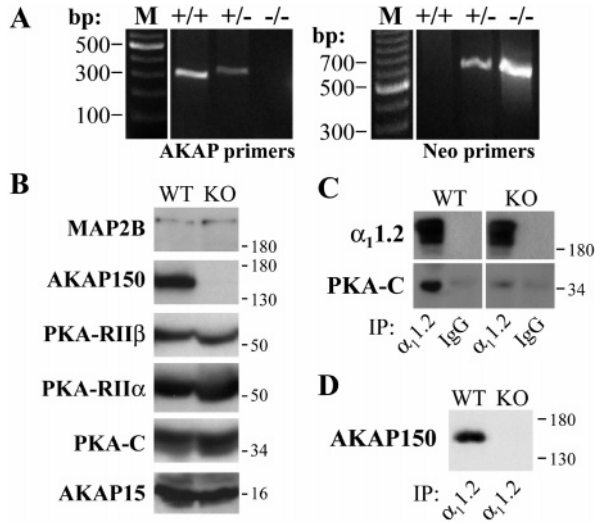

FIGURE 5: Co-immunoprecipitation of PKA with $Ca_v1.2$ is strongly reduced in AKAP150 KO mice. (A) Genotyping of wild-type and AKAP150 KO mice. AKAP150 was targeted for disruption with a neomycin phosphotransferase cassette that displaces the AKAP150 coding sequence. Primers specific for endogenous AKAP150 and for the neomycin marker were used to amplify genomic DNA. AKAP150 is present in wild-type (left panel; +/+) and heterozygous (+/−) mice but deficient in the knockout animals (−/−). The neomycin-positive PCR product indicates the presence of an AKAP150-disrupted allele (right panel; +/−, −/−). (B) PKA and other AKAP expression levels remain unaltered in AKAP150 KO mice. Forebrains of C57black/6 wild-type (WT) and congenic AKAP150 KO mice were harvested and homogenized as described in Experimental Procedures. Extracts from Triton X-100 solubilized membranes were separated via SDS−PAGE, and immunoblots were probed for AKAP150, MAP2B, AKAP15, PKA regulatory RIIα or RIIβ subunit, or PKA catalytic C subunit. AKAP150 KO mice showed no changes in the relative amount of these proteins compared to wild-type mice other than elimination of AKAP150. (C, D) Reduced interaction between PKA and $\alpha_1$1.2 in the absence of AKAP150. The $\alpha_1$1.2 subunit of $Ca_v1.2$ or nonspecific proteins were immunoprecipitated from the Triton X-100 extracts used above with 10 μg of anti-$\alpha_1$1.2 or control IgG, respectively. Immunoblots were probed with antibodies against PKA-C, $\alpha_1$1.2 (C) or AKAP150 (D). The left and right panels for each probing in (B) are from the same immunoblot exposure. PKA-C coprecipitation was substantially reduced to 20% of wild-type association levels. The amount of anti-$\alpha_1$1.2 signal illustrates that similar amounts of $\alpha_1$1.2 were isolated in $\alpha_1$1.2 immunoprecipitates from wild-type and KO animals.

that interact with or are in the immediate vicinity of $Ca_v1.2$ cannot substitute for AKAP150 as knockout of AKAP150 eliminates the isoproterenol-dependent increase in $\alpha_1$1.2 phosphorylation seen in wild-type animals.

Physiological Relevance of $\alpha_1$1.2 Serine 1928 Phosphorylation. We provide the first in vivo evidence that $\alpha_1$1.2 is phosphorylated on serine 1928 in response to β-adrenergic stimuli (Figure 1). The functional relevance of serine 1928 phosphorylation by PKA and β-adrenergic regulation, however, has been controversial. Much of these disparate data comes from ectopic expression of $Ca_v1.2$ in cultured cells. In agreement with our data, expression of serine 1928 to alanine-mutated $\alpha_1$1.2 in HEK cells prevented 8-Br-cAMP and forskolin mediated increases in channel activity (*30*, *76*). However, a follow-up study found that truncation of the $\alpha_1$1.2 C-terminus upstream of serine 1928 at residue 1905 allowed for a PKA-dependent increase in activity (*25*). Recently, Ganesan et al. (*77*) used adenoviral transduction of dihydropyridine-insensitive $\alpha_1$1.2 alleles in cardiomyocytes. Truncated $\alpha_1$1.2 at position 1905 blunted the isoproterenol response compared to wild type. Mutation of serine 1928 to alanine led to a modest but consistent decrease of approximately 30% in calcium current upregulation by

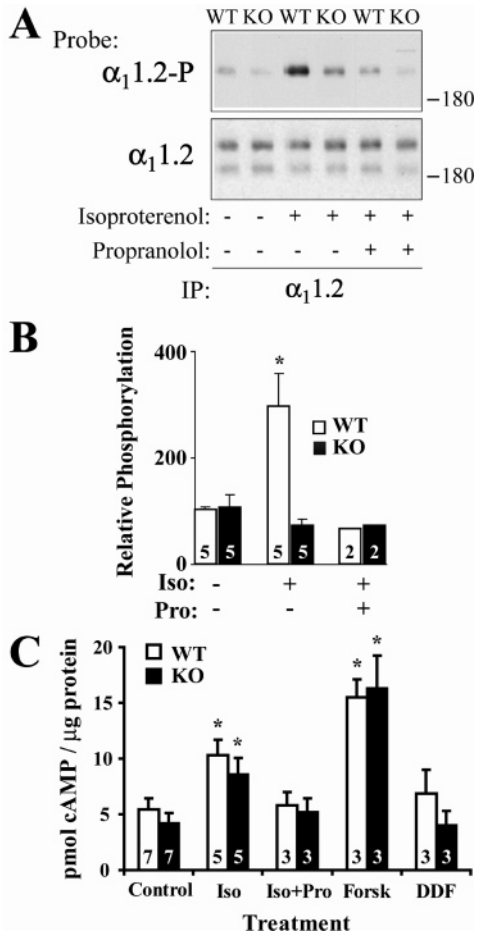

FIGURE 6: AKAP150 is required for isoproterenol-induced phosphorylation of serine 1928 on the $\alpha_1$1.2 subunit of hippocampal $Ca_v1.2$ in vivo. (A) Sample Western blot showing the increase in serine 1928 phosphorylation upon isoproterenol administration in wild-type (WT) but not AKAP150 KO animals. C57black/6 WT and congenic AKAP150 KO mice were injected with either vehicle (1 mL of PBS), (−) isoproterenol (10 mg/kg), or (−)-isoproterenol plus (*S*)-(−)-propranolol (10 mg/kg) as indicated. After 20 min, mice were decapitated and brain hippocampi homogenized in 1% Triton X-100 solubilization buffer. Insoluble material was removed by ultracentrifugation and $\alpha_1$1.2 immunoprecipitated with the anti-$\alpha_1$1.2 antibody. Immunoblots were probed with anti-$\alpha_1$1.2-P followed by anti-$\alpha_1$1.2 to account for any changes in the amount of $\alpha_1$1.2 immunoprecipitated. (B) Quantification of $\alpha_1$1.2 serine 1928 phosphorylation. The relative signal of anti-$\alpha_1$1.2-P to anti-$\alpha_1$1.2 for each sample was determined via densitometry for the full-length form of $\alpha_1$1.2. Isoproterenol does not increase the serine 1928 phosphorylation level in AKAP150 KO mice, which is significantly different from the serine 1928 phosphorylation level of isoproterenol-treated wild-type mice (*, $p < 0.05$, SEM, *t*-test). (C) Regulation of cAMP production is independent of AKAP150. Acute cortical slices were prepared from wild-type and KO mice and treated with 3 μM propranolol, as indicated, or buffer for 30 min. Vehicle, 3 μM isoproterenol, 50 μM forskolin, or 50 μM dideoxyforskolin (DDF) was then added as indicated for 10 min. Slices were immediately frozen and homogenized with 0.1 N HCl and lysates used in a cAMP assay as described in Experimental Procedures. Isoproterenol and forskolin stimulated cAMP production significantly in both wild-type (white bars) and AKAP150 KO slices (black bars) (*, $p < 0.05$, SEM, *t*-test). There was no significant difference between wild-type and KO values. The number of experiments per treatment is indicated within the bars.

isoproterenol, although this decrease did not reach statistical significance. However, as elegant as it is, the viral infection system by Ganesan et al. (*77*) only partially reconstitutes the regulation of $Ca_v1.2$ by β-adrenergic. In native myocytes isoproterenol increased calcium current by 300% whereas in myocytes overexpressing $\alpha_1 1.2$ the increase was only 50%. The role of serine 1928 phosphorylation might have been blunted in that system.

In support of a critical role of serine 1928 phosphorylation in the regulation of $Ca_v1.2$ activity, mutation of neuronal rat $\alpha_1 1.2$ on serine 1901 (equivalent to serine 1928 from the rabbit cardiac nomenclature) abolished the forskolin-dependent increase in calcium currents in BHK6 cells (*78*). Similarly, a recent publication provided further evidence that mutating serine 1928 to alanine substantially inhibits PKA-mediated regulation of $Ca_v1.2$ (*76*). Perhaps the functional role of serine 1928 phosphorylation will be resolved through the generation and subsequent analysis of transgenic mice mutated at this residue.

$Ca_v1.2$ Binds Three Different AKAPs in Neurons: AKAP150, AKAP15, and MAP2B. Anchoring of PKA ensures spatial proximity to its substrates for their effective phosphorylation, thereby promoting phosphorylation of selected substrates (*34*−*36*) including $Ca_v1.2$ (*30*, *40*). We identified three different AKAPs that co-immunoprecipitate with the $\alpha_1 1.2$ subunit of $Ca_v1.2$ from rodent brain extracts: AKAP150, AKAP15, and MAP2B (Figures 2 and 3). Earlier results demonstrated a direct interaction of AKAP15 with a leucine zipper-like motif near the C-terminus of $\alpha_1 1.2$ (*40*). This interaction likely constitutes the main PKA anchoring mechanism for $Ca_v1.2$ in the heart. We now show that, in contrast to AKAP15, AKAP150 and MAP2B bind to three different sites, the N-terminus, the I−II loop, and the distal region of the long C-terminus as represented by the CT-7 fusion protein (Figure 4). Auxiliary Ca^{2+} channel β subunits show a similar binding pattern, i.e., interact with regions in the N-terminus, loop I−II, and the C-terminus (*79*, *80*). Similarly, the G$\beta\gamma$ dimer of trimeric G proteins can also bind to the N-terminus, loop I−II, and the C-terminus (*81*). Collectively, these observations argue that the N-terminus, loop I−II, and the C-terminus may be in close proximity to each other in the folded channel as proposed earlier (e.g., ref *79*) and participate in multiple protein interactions.

With respect to the $\alpha_1 1.2$ C-terminal binding region for AKAP75/79/150, the last 142 residues of rabbit $\alpha_1 1.2$ (CT-7) and the last 117 residues of rat $\alpha_1 1.2$ (CT-E) interact with GST-AKAP75 (Figure 4). The CT-E sequence is 80% identical to CT-7. The difference in relative affinities between the two fragments for GST-AKAP75 may be due to either the difference in the sequences between the two species or the additional 25 residues covered by CT-7. Both of these constructs contain the leucine zipper-like segment that interacts with AKAP15 (*40*); however, AKAP75/79/150 does not have an obvious leucine zipper-like sequence. Despite several tests addressing this issue, we have no evidence that AKAP75/79/150 can interact with this motif.

AKAP150 Is the Main AKAP for Recruiting PKA to $Ca_v1.2$ in Neurons. Although three different AKAPs are specifically associated with $Ca_v1.2$ in brain, knockout of AKAP150 (Figure 5A,C) results in a near loss of co-immunoprecipitation of PKA with $Ca_v1.2$ (Figure 5B). Protein levels of AKAP15, MAP2B, and, importantly, PKA subunits remained unaltered in the KO mice (Figure 5B). Accordingly, decreased co-immunoprecipitation of PKA with $Ca_v1.2$ in AKAP150 KO mice is not due to reduced availability of PKA. We further demonstrate that knockout of AKAP150 eliminates phosphorylation of $Ca_v1.2$ on serine 1928 upon β-adrenergic stimulation (Figure 6). Therefore, neither AKAP15 nor MAP2B can compensate for linking PKA to $Ca_v1.2$ in brain in the AKAP150 KO mice. We conclude that AKAP150 is the prevailing and most critical AKAP for recruiting PKA to $Ca_v1.2$ in brain.

Specificity of AKAPs in Signaling by PKA despite Their Spatial Proximity. PKA anchoring supports effective and specific signaling with what appears to be a remarkable spatial restriction with respect to the AKAPs involved. Considering that $Ca_v1.2$ is near other AKAP-binding proteins in dendritic spines and less than 100 nm away from ryanodine receptors in myocytes, PKA must be anchored immediately next to defined phosphorylation sites for their effective phosphorylation. Several AKAPs including Yotiao, mAKAP, MAP2C, and AKAP220 did not co-immunoprecipitate with $Ca_v1.2$ from brain extracts (Figures 2 and 3) (*26*). Yotiao links PKA to the NMDA receptor at postsynaptic sites (*72*, *73*) where $Ca_v1.2$ is also concentrated (*31*, *50*). Despite the proximity of the NMDA receptor complex and hence Yotiao to $Ca_v1.2$, PKA anchored by Yotiao is obviously not able to substantially contribute to $Ca_v1.2$ phosphorylation by PKA upon β-adrenergic activation, as β-adrenergic stimulation of $Ca_v1.2$ phosphorylation is completely eliminated in the AKAP150 KO mice (Figure 6). Analogous considerations apply to mAKAP which is localized along the Z lines in cardiomyocytes (*82*) and links PKA to the cardiac ryanodine receptor (*66*). Functional studies indicate that PKA uses two different AKAPs in the heart. AKAP15 and mAKAP link PKA to $Ca_v1.2$ and the ryanodine receptor, respectively (*40*, *66*). It appears that PKA anchored at $Ca_v1.2$ cannot support effective phosphorylation of ryanodine receptors by PKA and vice versa (*40*).

AKAPs may aid in PKA substrate specificity through steric orientation of the C subunit for optimal access. In vitro cAMP binding to the PKA regulatory R subunit dimer leads to dissociation and concomitant activation of the catalytic C subunit, which is inhibited in the R−C complex. Release of the C subunit should facilitate phosphorylation of neighboring protein complexes, thereby reducing selectivity of substrate phosphorylation by its anchoring unless there are additional anchoring mechanisms for the C subunit. In fact, more recent evidence indicates that C subunits can phosphorylate substrates without completely dissociating from RII subunits in the presence of cAMP (*83*, *84*). However, more work is necessary to better understand C subunit behavior upon addition of cAMP.

Localized Signaling from the β_2-Adrenergic Receptor to $Ca_v1.2$. Spatial restrictions and specific AKAP−PKA substrate interactions likely contribute to the specificity with which regulatory signaling pathways upstream of PKA are linked to phosphorylation of PKA substrates. It is necessary that the G protein coupled receptors that trigger $Ca_v1.2$ regulation via PKA are in close proximity to and have higher selectivity for the $Ca_v1.2$−PKA complex compared to receptors with little or no contribution to $Ca_v1.2$ regulation. One example is the β_2-AR, which forms a signaling complex with $Ca_v1.2$ (*50*). This complex contains the trimeric G_S

protein and adenylyl cyclase, which mediate signaling from the β_2-AR to PKA (*50*). Stimulation of β_2-ARs increases Ca^{2+} influx into dendritic spines through L-type Ca^{2+} channels (*16*), which are primarily $Ca_v1.2$ (*2*, *19*, *21*, *31*, *50*). The β_2-AR and $Ca_v1.2$ are coclustered at dendritic spines, which constitute postsynaptic sites of glutamatergic synapses (*31*, *50*). They also form co-clusters at the plasma membrane of neuronal cell bodies, which are juxtaposed to presynaptic sites and presumably reflect GABAergic synapses (*50*). Cell-attached recordings of L-type channel activity revealed highly localized signaling from the β_2-AR to L-type channels at the plasma membrane of the neuronal soma (*50*). Accordingly, the assembly of the β_2-AR−G_S protein−adenylyl cyclase−AKAP150−PKA−$Ca_v1.2$ signaling complex may underlie localized and thereby specific signaling from the β_2-AR to $Ca_v1.2$. This signaling complex also includes the phosphatase PP2A, which binds to $\alpha_1$1.2 downstream of serine 1928 for effective and fast reversal of its phosphorylation (*28*, *58*).

ACKNOWLEDGMENT

The authors thank Drs. W. A. Catterall, University of Washington, Seattle, WA, for providing the anti-AKAP15 antibody, J. W. Tracy, University of Wisconsin, Madison, WI, for the anti-GST antibody, C. S. Rubin, Albert Einstein College of Medicine, Bronx, NY, for the anti-PKA Cα antibody, and M. Marlene Hosey, Northwestern University, Chicago, IL, for the expression constructs for GST-CT-1, -5, and -7.

REFERENCES

1. Helton, T. D., Xu, W., and Lipscombe, D. (2005) Neuronal L-type calcium channels open quickly and are inhibited slowly, *J. Neurosci. 25*, 10247−10251.
2. Moosmang, S., Haider, N., Klugbauer, N., Adelsberger, H., Langwieser, N., Muller, J., Stiess, M., Marais, E., Schulla, V., Lacinova, L., Goebbels, S., Nave, K. A., Storm, D. R., Hofmann, F., and Kleppisch, T. (2005) Role of hippocampal $Ca_v1.2$ Ca^{2+} channels in NMDA receptor-independent synaptic plasticity and spatial memory, *J. Neurosci. 25*, 9883−9892.
3. Marrion, N. V., and Tavalin, S. T. (1998) Selective activation of Ca^{2+}-activated K^+ channels by co-localized Ca^{2+} channels in hippocampal neurons, *Nature 395*, 900−905.
4. Bolshakov, V. Y., and Siegelbaum, S. A. (1994) Postsynaptic induction and presynaptic expression of hippocampal long-term depression, *Science 264*, 148−152.
5. Christie, B. R., Schexnayder, L. K., and Johnston, D. (1997) Contribution of voltage-gated Ca^{2+} channels to homosynaptic long-term depression in the CA1 region in vitro, *J. Neurophysiol. 77*, 1651−1655.
6. Grover, L. M., and Teyler, T. J. (1990) Two components of long-term potentiation induced by different patterns of afferent activation, *Nature 347*, 477−479.
7. Wang, H. X., Gerkin, R. C., Nauen, D. W., and Bi, G. Q. (2005) Coactivation and timing-dependent integration of synaptic potentiation and depression, *Nat. Neurosci. 8*, 187−193.
8. Dolmetsch, R. E., Pajvani, U., Fife, K., Spotts, J. M., and Greenberg, M. E. (2001) Signaling to the nucleus by an L-type calcium channel-calmodulin complex through the MAP kinase pathway, *Science 294*, 333−339.
9. Ghosh, A., and Greenberg, M. E. (1995) Calcium signaling in neurons: molecular mechanisms and cellular consequences, *Science 268*, 239−247.
10. Bean, B. P., Nowycky, M. C., and Tsien, R. W. (1984) β-Adrenergic modulation of calcium channels in frog ventricular heart cells, *Nature 307*, 371−375.
11. De Jongh, K. S., Murphy, B. J., Colvin, A. A., Hell, J. W., Takahashi, M., and Catterall, W. A. (1996) Specific phosphorylation of a site in the full length form of the α1 subunit of the cardiac L-type calcium channel by adenosine 3′,5′-cyclic monophosphate-dependent protein kinase, *Biochemistry 35*, 10392−10402.
12. Reuter, H. (1983) Calcium channel modulation by neurotransmitters, enzymes and drugs, *Nature 301*, 569−574.
13. Fisher, R., and Johnston, D. (1990) Differential modulation of single voltage-gated calcium channels by cholinergic and adrenergic agonists in adult hippocampal neurons, *J. Neurophysiol. 64*, 1291−1302.
14. Gray, R., and Johnston, D. (1987) Noradrenaline and beta-adrenoceptor agonists increase activity of voltage-dependent calcium channels in hippocampal neurons, *Nature 327*, 620−622.
15. Gross, R. A., Uhler, M. D., and Macdonald, R. L. (1990) The cyclic AMP-dependent protein kinase catalytic subunit selectively enhances calcium currents in rat nodose neurones, *J. Physiol. 429*, 483−496.
16. Hoogland, T. M., and Saggau, P. (2004) Facilitation of L-type Ca^{2+} channels in dendritic spines by activation of beta2 adrenergic receptors, *J. Neurosci. 24*, 8416−8427.
17. Surmeier, D. J., Bargas, J., Hemmings, H. C., Jr., Nairn, A. C., and Greengard, P. (1995) Modulation of calcium currents by a D1 dopaminergic protein kinase/phosphatase cascade in rat neostriatal neurons, *Neuron 14*, 385−397.
18. Ertel, E. A., Campbell, K. P., Harpold, M. M., Hofmann, F., Mori, Y., Perez-Reyes, E., Schwartz, A., Snutch, T. P., Tanabe, T., Birnbaumer, L., Tsien, R. W., and Catterall, W. A. (2000) Nomenclature of voltage-gated calcium channels, *Neuron 25*, 533−535.
19. Hell, J. W., Westenbroek, R. E., Warner, C., Ahlijanian, M. K., Prystay, W., Gilbert, M. M., Snutch, T. P., and Catterall, W. A. (1993) Identification and differential subcellular localization of the neuronal class C and class D L-type calcium channel α1 subunits, *J. Cell Biol. 123*, 949−962.
20. Hell, J. W., Yokoyama, C. T., Wong, S. T., Warner, C., Snutch, T. P., and Catterall, W. A. (1993) Differential phosphorylation of two size forms of the neuronal class C L-type calcium channel α1 subunit, *J. Biol. Chem. 268*, 19451−19457.
21. Sinnegger-Brauns, M. J., Hetzenauer, A., Huber, I. G., Renstrom, E., Wietzorrek, G., Berjukov, S., Cavalli, M., Walter, D., Koschak, A., Waldschutz, R., Hering, S., Bova, S., Rorsman, P., Pongs, O., Singewald, N., and Striessnig, J. J. (2004) Isoform-specific regulation of mood behavior and pancreatic beta cell and cardiovascular function by L-type Ca^{2+} channels, *J. Clin. Invest. 113*, 1430−1439.
22. Catterall, W. A. (2000) Structure and regulation of voltage-gated Ca^{2+} channels, *Annu. Rev. Cell Dev. Biol. 16*, 521−555.
23. Viard, P., Butcher, A. J., Halet, G., Davies, A., Nurnberg, B., Heblich, F., and Dolphin, A. C. (2004) PI3K promotes voltage-dependent calcium channel trafficking to the plasma membrane, *Nat. Neurosci. 7*, 939−946.
24. Sculptoreanu, A., Rotman, E., Takahashi, M., Scheuer, T., and Catterall, W. A. (1993) Voltage-dependent potentiation of the activity of cardiac L-type calcium channel alpha 1 subunits due to phosphorylation by cAMP-dependent protein kinase, *Proc. Natl. Acad. Sci. U.S.A. 90*, 10135−10139.
25. Bunemann, M., Gerhardstein, B. L., Gao, T., and Hosey, M. M. (1999) Functional regulation of L-type calcium channels via protein kinase A-mediated phosphorylation of the beta(2) subunit, *J. Biol. Chem. 274*, 33851−33854.
26. Davare, M. A., Dong, F., Rubin, C. S., and Hell, J. W. (1999) The A-kinase anchor protein MAP2B and cAMP-dependent protein kinase are associated with class C L-type calcium channels in neurons, *J. Biol. Chem. 274*, 30280−30287.
27. Davare, M. A., and Hell, J. W. (2003) Increased phosphorylation of the neuronal L-type Ca(2+) channel Ca(v)1.2 during aging, *Proc. Natl. Acad. Sci. U.S.A. 100*, 16018−16023.
28. Davare, M. A., Horne, M. C., and Hell, J. W. (2000) Protein phosphatase 2A is associated with class C L-type calcium channels ($Ca_v1.2$) and antagonizes channel phosphorylation by cAMP-dependent protein kinase, *J. Biol. Chem. 275*, 39710−39717.
29. Hell, J. W., Yokoyama, C. T., Breeze, L. J., Chavkin, C., and Catterall, W. A. (1995) Phosphorylation of presynaptic and postsynaptic calcium channels by cAMP-dependent protein kinase in hippocampal neurons, *EMBO J. 14*, 3036−3044.
30. Gao, T., Yatani, A., Dell'Acqua, M. L., Sako, H., Green, S. A., Dascal, N., Scott, J. D., and Hosey, M. M. (1997) cAMP-dependent regulation of cardiac L-type Ca^{2+} channels requires membrane targeting of PKA and phosphorylation of channel subunits, *Neuron 19*, 185−196.

31. Hell, J. W., Westenbroek, R. E., Breeze, L. J., Wang, K. K. W., Chavkin, C., and Catterall, W. A. (1996) N-methyl-D-aspartate receptor-induced proteolytic conversion of postsynaptic class C L-type calcium channels in hippocampal neurons, *Proc. Natl. Acad. Sci. U.S.A. 93*, 3362−3367.
32. Hell, J. W., Westenbroek, R. E., Elliott, E. M., and Catterall, W. A. (1994) Differential phosphorylation, localization, and function of distinct α1 subunits of neuronal calcium channels. Two size forms for class B, C, and D α1 subunits with different COOH-termini, *Ann. N.Y. Acad. Sci. 747*, 282−293.
33. Wei, X., Neely, A., Lacerda, A. E., Olcese, R., Stefani, E., Perez-Reyes, E., and Birnbaumer, L. (1994) Modification of Ca^{2+} channel activity by deletions at the carboxyl terminus of the cardiac alpha 1 subunit, *J. Biol. Chem. 269*, 1635−1640.
34. Gray, P. C., Scott, J. D., and Catterall, W. A. (1998) Regulation of ion channels by cAMP-dependent protein kinase and A-kinase anchoring proteins, *Curr. Opin. Neurobiol. 8*, 330−334.
35. Rubin, C. S. (1994) A kinase anchor proteins and the intracellular targeting of signals carried by cyclic AMP, *Biochim. Biophys. Acta 1224*, 467−479.
36. Wong, W., and Scott, J. D. (2004) AKAP signalling complexes: focal points in space and time, *Nat. Rev. Mol. Cell. Biol. 5*, 959−970.
37. Hoshi, N., Langeberg, L. K., and Scott, J. D. (2005) Distinct enzyme combinations in AKAP signalling complexes permit functional diversity, *Nat. Cell. Biol. 7*, 1066−1073.
38. Rosenmund, C., Carr, D. W., Bergeson, S. E., Nilaver, G., Scott, J. D., and Westbrook, G. L. (1994) Anchoring of protein kinase A is required for modulation of AMPA/kainate receptors on hippocampal neurons, *Nature 368*, 853−856.
39. Johnson, B. D., Scheuer, T., and Catterall, W. A. (1994) Voltage-dependent potentiation of L-type Ca^{2+} channels in skeletal muscle cells requires anchored cAMP-dependent protein kinase, *Proc. Natl. Acad. Sci. U.S.A. 91*, 11492−11496.
40. Hulme, J. T., Lin, T. W., Westenbroek, R. E., Scheuer, T., and Catterall, W. A. (2003) Beta-adrenergic regulation requires direct anchoring of PKA to cardiac $Ca_v1.2$ channels via a leucine zipper interaction with A kinase-anchoring protein 15, *Proc. Natl. Acad. Sci. U.S.A. 100*, 13093−13098.
41. Vallee, R. B., DiBartolomeis, M. J., and Theurkauf, W. E. (1981) A protein kinase bound to the projection portion of MAP 2 (microtubule-associated protein 2), *J. Cell Biol. 90*, 568−576.
42. Fraser, I. D. C., Tavalin, S. J., Lester, L. B., Langeberg, L. K., Westphal, A. M., Dean, R. A., Marrion, N. V., and Scott, J. D. (1998) A novel lipid-anchored A-kinase anchoring protein facilitates cAMP-responsive membrane events, *EMBO J. 17*, 2261−2272.
43. Gray, P. C., Johnson, B. D., Westenbroek, R. E., Hays, L. G., Yates, J. R., III, Scheuer, T., Catterall, W. A., and Murphy, B. J. (1998) Primary structure and function of an A kinase anchoring protein associated with calcium channels, *Neuron 20*, 1017−1026.
44. Gomez, L. L., Alam, S., Smith, K. E., Horne, E., and Dell'Acqua, M. L. (2002) Regulation of A-kinase anchoring protein 79/150-cAMP-dependent protein kinase postsynaptic targeting by NMDA receptor activation of calcineurin and remodeling of dendritic actin, *J. Neurosci. 22*, 7027−7044.
45. Gorski, J. A., Gomez, L. L., Scott, J. D., and Dell'Acqua, M. L. (2005) Association of an A-kinase-anchoring protein signaling scaffold with cadherin adhesion molecules in neurons and epithelial cells, *Mol. Biol. Cell 16*, 3574−3590.
46. Colledge, M., Dean, R. A., Scott, G. K., Langeberg, L. K., Huganir, R. L., and Scott, J. D. (2000) Targeting of PKA to glutamate receptors through a MAGUK-AKAP complex, *Neuron 27*, 107−119.
47. Mammen, A. L., Kameyama, K., Roche, K. W., and Huganir, R. L. (1997) Phosphorylation of the α-amino-3-hydroxy-5-methylisoxazole-4-propionic acid receptor GluR1 subunit by calcium/calmodulin-dependent kinase II, *J. Biol. Chem. 272*, 32528−32533.
48. Roche, K. W., O'Brien, R. J., Mammen, A. L., Bernhardt, J., and Huganir, R. L. (1996) Characterization of multiple phosphorylation sites on the AMPA receptor GluR1 subunit, *Neuron 16*, 1179−1188.
49. Tavalin, S. J., Colledge, M., Hell, J. W., Langeberg, L. K., Huganir, R. L., and Scott, J. D. (2002) Regulation of GluR1 by the A-kinase anchoring protein 79 (AKAP79) signaling complex shares properties with long-term depression, *J. Neurosci. 22*, 3044−3051.
50. Davare, M. A., Avdonin, V., Hall, D. D., Peden, E. M., Burette, A., Weinberg, R. J., Horne, M. C., Hoshi, T., and Hell, J. W. (2001) A beta2 adrenergic receptor signaling complex assembled with the Ca^{2+} channel $Ca_v1.2$, *Science 293*, 98−101.
51. Altier, C., Dubel, S. J., Barrere, C., Jarvis, S. E., Stotz, S. C., Spaetgens, R. L., Scott, J. D., Cornet, V., De Waard, M., Zamponi, G. W., Nargeot, J., and Bourinet, E. (2002) Trafficking of L-type calcium channels mediated by the postsynaptic scaffolding protein AKAP79, *J. Biol. Chem. 277*, 33598−33603.
52. Burton, K. A., Treash-Osio, B., Muller, C. H., Dunphy, E. L., and McKnight, G. S. (1999) Deletion of type IIalpha regulatory subunit delocalizes protein kinase A in mouse sperm without affecting motility or fertilization, *J. Biol. Chem. 274*, 24131−24136.
53. Leonard, A. S., Davare, M. A., Horne, M. C., Garner, C. C., and Hell, J. W. (1998) SAP97 is associated with the α-amino-3-hydroxy-5-methylisoxazole-4-propionic acid receptor GluR1 subunit, *J. Biol. Chem. 273*, 19518−19524.
54. Liu, G., Shi, J., Yang, L., Cao, L., Park, S. M., Cui, J., and Marx, S. O. (2004) Assembly of a Ca(2+)-dependent BK channel signaling complex by binding to beta2 adrenergic receptor, *EMBO J. 23*, 2196−2205.
55. Nauert, J. B., Rigas, J. D., and Lester, L. B. (2003) Identification of an IQGAP1/AKAP79 complex in beta-cells, *J. Cell. Biochem. 90*, 97−108.
56. Ruehr, M. L., Russell, M. A., Ferguson, D. G., Bhat, M., Ma, J., Damron, D. S., Scott, J. D., and Bond, M. (2003) Targeting of protein kinase A by muscle A kinase-anchoring protein (mAKAP) regulates phosphorylation and function of the skeletal muscle ryanodine receptor, *J. Biol. Chem. 278*, 24831−24836.
57. Schulze, D. H., Muqhal, M., Lederer, W. J., and Ruknudin, A. M. (2003) Sodium/calcium exchanger (NCX1) macromolecular complex, *J. Biol. Chem. 278*, 28849−28855.
58. Hall, D. D., Feekes, J. A., ArachchigeDon, A. S., Shi, M., Hamid, J., Chen, L., Strack, S., Zamponi, G. W., Horne, M. C., and Hell, J. W. (2006) Binding of protein phosphatase 2A to the L-type calcium channel $Ca_v1.2$ next to Ser1928, its main PKA site, is critical for Ser1928 dephosphorylation, *Biochemistry 45*, 3448−3459.
59. Snutch, T. P., Tomlinson, W. J., Leonard, J. P., and Gilbert, M. M. (1991) Distinct calcium channels are generated by alternative splicing and are differentially expressed in the mammalian CNS, *Neuron 7*, 45−57.
60. Li, Y., Ndubuka, C., and Rubin, C. S. (1996) A kinase anchor protein 75 targets regulatory (RII) subunits of cAMP-dependent protein kinase II to the cortical actin cytoskeleton in non-neuronal cells, *J. Biol. Chem. 271*, 16862−16869.
61. Gao, T., Cuadra, A. E., Ma, H., Bunemann, M., Gerhardstein, B. L., Cheng, T., Eick, R. T., and Hosey, M. M. (2001) C-terminal fragments of the alpha 1C ($Ca_v1.2$) subunit associate with and regulate L-type calcium channels containing C-terminal-truncated alpha 1C subunits, *J. Biol. Chem. 276*, 21089−21097.
62. Leonard, A. S., Lim, I. A., Hemsworth, D. E., Horne, M. C., and Hell, J. W. (1999) Calcium/calmodulin-dependent protein kinase II is associated with the *N*-methyl-D-aspartate receptor, *Proc. Natl. Acad. Sci. U.S.A. 96*, 3239−3244.
63. Li, Y., and Rubin, C. S. (1995) Mutagenesis of the regulatory subunit (RII beta) of cAMP-dependent protein kinase II beta reveals hydrophobic amino acids that are essential for RII beta dimerization and/or anchoring RII beta to the cytoskeleton, *J. Biol. Chem. 270*, 1935−1944.
64. Kapiloff, M. S., Schillace, R. V., Westphal, A. M., and Scott, J. D. (1999) mAKAP: an A-kinase anchoring protein targeted to the nuclear membrane of differentiated myocytes, *J. Cell Sci. 112* (Part 16), 2725−2736.
65. Gray, P. C., Tibbs, V. C., Catterall, W. A., and Murphy, B. J. (1997) Identification of a 15-kDa cAMP-dependent protein kinase-anchoring protein associated with skeletal muscle L-type calcium channels, *J. Biol. Chem. 272*, 6297−6302.
66. Marx, S. O., Reiken, S., Hisamatsu, Y., Gaburjakova, M., Gaburjakova, J., Yang, Y. M., Rosemblit, N., and Marks, A. R. (2001) Phosphorylation-dependent regulation of ryanodine receptors: a novel role for leucine/isoleucine zippers, *J. Cell Biol. 153*, 699−708.
67. Martone, M. E., Alba, S. A., Edelman, V. M., Airey, J. A., and Ellisman, M. H. (1997) Distribution of inositol-1,4,5-trisphosphate and ryanodine receptors in rat neostriatum, *Brain Res. 756*, 9−21.
68. Sharp, A. H., McPherson, P. S., Dawson, T. M., Aoki, C., Campbell, K. P., and Snyder, S. H. (1993) Differential immunohistochemical localization of inositol 1,4,5-trisphosphate- and

ryanodine-sensitive Ca^{2+} release channels in rat brain, *J. Neurosci. 13*, 3051−3063.
69. Emptage, N., Bliss, T. V., and Fine, A. (1999) Single synaptic events evoke NMDA receptor-mediated release of calcium from internal stores in hippocampal dendritic spines, *Neuron 22*, 115−124.
70. Raymond, C. R., and Redman, S. J. (2006) Spatial segregation of neuronal calcium signals encodes different forms of LTP in rat hippocampus, *J. Physiol. 570*, 97−111.
71. Chavis, P., Fagni, L., Lansman, J. B., and Bockaert, J. (1996) Functional coupling between ryanodine receptors and L-type calcium channels in neurons, *Nature 382*, 719−722.
72. Lin, J. W., Wyszynski, M., Madhavan, R., Sealock, R., Kim, J. U., and Sheng, M. (1998) Yotiao, a novel protein of neuromuscular junction and brain that interacts with specific splice variants of NMDA receptor subunit NR1, *J. Neurosci. 18*, 2017−2027.
73. Westphal, R. S., Tavalin, S. J., Lin, J. W., Alto, N. M., Fraser, I. D. C., Langeberg, L. K., Sheng, M., and Scott, J. D. (1999) Regulation of NMDA receptors by an associated phosphatase-kinase signaling complex, *Science 285*, 93−96.
74. Fraser, I. D., Cong, M., Kim, J., Rollins, E. N., Daaka, Y., Lefkowitz, R. J., and Scott, J. D. (2000) Assembly of an A kinase-anchoring protein-beta(2)-adrenergic receptor complex facilitates receptor phosphorylation and signaling, *Curr. Biol. 10*, 409−412.
75. Bauman, A. L., Soughayer, J., Nguyen, B. T., Willoughby, D., Carnegie, G. K., Wong, W., Hoshi, N., Langeberg, L. K., Cooper, D. M. F., Dessauer, C. W., and Scott, J. D. (2006) Dynamic regulation of cAMP synthesis through anchored PKA-adenylyl cyclase V/VI complexes, *Mol. Cell 23*, 925−931.
76. Gui, P., Wu, X., Ling, S., Stotz, S. C., Winkfein, R. J., Wilson, E., Davis, G. E., Braun, A. P., Zamponi, G. W., and Davis, M. J. (2006) Integrin receptor activation triggers converging regulation of $Ca_v1.2$ calcium channels by c-Src and protein kinase A pathways, *J. Biol. Chem. 281*, 14015−14025.
77. Ganesan, A. N., Maack, C., Johns, D. C., Sidor, A., and O'Rourke, B. (2006) {beta}-Adrenergic stimulation of L-type Ca^{2+} channels in cardiac myocytes requires the distal carboxyl terminus of {alpha}1C but not serine 1928, *Circ. Res. 98*, e11−18.
78. Naguro, I., Nagao, T., and Adachi-Akahane, S. (2001) Ser1901 of [alpha]1C subunit is required for the PKA-mediated enhancement of L-type Ca^{2+} channel currents but not for the negative shift of activation, *FEBS Lett. 489*, 87−91.
79. Walker, D., Bichet, D., Geib, S., Mori, E., Cornet, V., Snutch, T. P., Mori, Y., and De Waard, M. (1999) A new beta subtype-specific interaction in alpha1A subunit controls P/Q-type Ca^{2+} channel activation, *J. Biol. Chem. 274*, 12383−12390.
80. Walker, D., and De Waard, M. (1998) Subunit interaction sites in votage-dependent Ca^{2+} channels: Role in channel function, *Trends Neurosci. 21*, 148−154.
81. De Waard, M., Hering, J., Weiss, N., and Feltz, A. (2005) How do G proteins directly control neuronal Ca^{2+} channel function?, *Trends Pharmacol. Sci. 26*, 427−436.
82. Yang, J., Drazba, J. A., Ferguson, D. G., and Bond, M. (1998) A-kinase anchoring protein 100 (AKAP100) is localized in multiple subcellular compartments in the adult rat heart, *J. Cell Biol. 142*, 511−522.
83. Vigil, D., Blumenthal, D. K., Brown, S., Taylor, S. S., and Trewhella, J. (2004) Differential effects of substrate on type I and type II PKA holoenzyme dissociation, *Biochemistry 43*, 5629−5636.
84. Yang, S., Fletcher, W. H., and Johnson, D. A. (1995) Regulation of cAMP-dependent protein kinase: enzyme activation without dissociation, *Biochemistry* 6267−6271.
85. Kindler, S., Schulz, B., Goedert, M., and Garner, C. C. (1990) Molecular structure of microtubule-associated protein 2b and 2c from rat brain, *J. Biol. Chem. 265*, 19679−19684.
86. Obar, R. A., Dingus, J., Bayley, H., and Vallee, R. B. (1989) The RII subunit of cAMP-dependent protein kinase binds to a common amino-terminal domain in microtubule-associated proteins 2A, 2B, and 2C, *Neuron 3*, 639−645.
87. Rubino, H. M., Dammerman, M., Shafit-Zagardo, B., and Erlichman, J. (1989) Localization and characterization of the binding site for the regulatory subunit of type II cAMP-dependent protein kinase on MAP2, *Neuron 3*, 631−638.
88. Lewis, S. A., Ivanov, I. E., Lee, G. H., and Cowan, N. J. (1989) Organization of microtubules in dendrites and axons is determined by a short hydrophobic zipper in microtubule-associated proteins MAP2 and tau, *Nature 342*, 498−505.
89. Lewis, S. A., Wang, D. H., and Cowan, N. J. (1988) Microtubule-associated protein MAP2 shares a microtubule binding motif with tau protein, *Science 242*, 936−939.

BI062217X